Vietnam Journal of Catalysis and Adsorption
Tạp chí xúc tác và hấp phụ Việt Nam

http://chemeng.hust.edu.vn/jca/

Synthesis, characterization of nano-sized ZnO prepared by a green, non chemical route

Nguyen Ngoc Thinh[1*], Nguyen Van Anh[2]

[1] *School of Chemical Engineering, Hanoi University of Science and Technology, Hanoi, VIETNAM*
[2] *Department of Environment Technology, Hanoi Metropolitan University, Hanoi, VIETNAM*
**Email: thinh.nguyenngoc@hust.edu.vn*

Vietnam – UK Researcher Link workshop

ARTICLE INFO

Received: 21/7/2018
Accepted: 18/8/2018

Keywords:
Zinc oxide, nanoparticles, green chemistry

ABSTRACT

In the present work, an eco-friendly method for the synthesis of nano- sized ZnO using the thermal decomposition of zinc acetate precursor without adding any chemical agents was studied. The synthesized materials were thoroughly characterized by various analytical tools such as XRD, FESEM & TEM. The XRD results indicated that the synthesized nano- sized ZnO had the pure wurtzite structure. The estimated crystallite sizes were of 33, 36, 38 and 42 nm for the products obtained from samples thermally decomposed at 450, 550, 650, 750^{0}C, respectively. The morphology of the nanoparticles was revealed to be affected by calcination temperature, causing the formation of both nanoparticles and nanorods with different size and shape.

Introduction

Metal oxide nanoparticles are of great interest due to their widespread applications. Employing their especial catalytic, electronic properties compared to bulk materials they have entered various different fields such as physics, chemistry, biology, medicine etc... The novel properties closely relate to their nano-sizes and their very large surface areas. Among currently used metal oxides, nano-sized zinc oxide is extensively applied as a photo catalyst in order to (1) remove pollutants, especially organic dyes; (2) develop advanced optic devices, sensors and so on. This is due to the fact that ZnO is a wide band gap (3.37 eV) semiconductor having significantly large excitation binding energy of 60 meV at room temperature and it has high transmittance and good electrical conductivity. In addition, ZnO is comparable to other metal oxides in its exceptional low cost [1], [2], [3]. There are various methods for the synthesis of ZnO nanoparticles such as: sol–gel, ultrasonic, microemulsion, thermal decomposition, spray pyrolysis, microwave-assisted techniques, chemical vapor deposition, hydrothermal and precipitation methods etc... However, high-cost equipment, complicated procedures, and/or elevated amounts of surfactants, oxidants, and toxic solvents are normally required. Besides, the aforementioned methods could barely generate large amounts of homogeneous products [2, 6, 8, 10, 12]. In this study, ZnO nanoparticles were prepared by direct decomposition of zinc acetate. The use of any additional chemical agents was, therefore, eliminated. The thermal decomposition of zinc acetate dihydrate was studied in advance by thermogravimetric analysis (TGA). The obtained ZnO nanoparticles were characterized by X-ray powder diffraction (XRD), transmission electron microscopy (TEM), and Field Emission Scanning Electron Microscopic (FESEM).

Experimental

The analytical grade zinc acetate dihydrate ($Zn(Ac)_2{\cdot}2H_2O$) was purchased from BDH (England) and directly used without further purification. The

thermal decomposition of zinc acetate dihydrate was studied by TGA (DSC131, Labsys TG/DSC1600, TMA, and Setaram, France) to determine its thermal stability and decomposition temperature. The TG curve of zinc acetate dihydrate was recorded in an air flow at the heating rate of 10°C min^{-1} from room temperature to 900^{0}C. Consequently, the temperature ranges from 450 to 750 for thermal decomposition of our samples were selected. In a typical procedure to prepare a sample, the amount of 3 g zinc acetate dihydrate ($Zn(Ac)_2{\cdot}2H_2O$) was grinded in an agate mortar. The samples were then transferred to closed porcelain crucibles and left in an oven (Nabertherm, Germany) for thermal decomposition at different temperature of 450^{0}C, 550^{0}C, 650^{0}C, and 750^{0}C within 4 hours with the temperature increasing rate of 10^0/min. The samples were allowed to cool down to room temperature and grinded in the agate mortar to obtain the final ZnO nanoparticles. Obtained products were named as ZnO-450, ZnO-550, ZnO-650 and ZnO-750 in accordance with the calcination temperatures of the samples.

The X-ray powder diffraction (XRD) patterns of the synthesized nanoparticles were provided using a Bruker D8 advanced X-ray diffractometer equipped with graphite monochromatized Cu Kα radiation (λ=1.5418 Å), scanning rate of 0.02 s^{-1}, scanning range of 20–75°. The FESEM characterization was performed on Hitachi S-4800 at 15 kV. Transmission electron microscopy (TEM) images were obtained with a JEOL JEM-1010 transmission electron microscope operating at an acceleration voltage of 200 kV.

Results and discussion

The TG and dTG (differential thermogravimetric) curves were provided in Figure 1. The thermal decomposition process started with approximately 15.72% weight loss that was presumed to be the thermal dehydration of zinc acetate dihydrate when the material became anhydrous zinc acetate. Further decomposition of anhydrous zinc acetate within the temperature region from 250 to 350^{0}C was accounted for the weight loss of 47.58%, which was higher than the calculated theoretical value of 46.5 wt. % if ZnO is the only residue. The difference of 1.08 wt. % might be due to the sublimation of zinc acetate species or the formation of other volatile zinc organic compositions [5]. The weight loss was no longer observed within the temperature ranges from 350 to 900^{0}C. This signaled the complete decomposition of the precursor at 350°C. Therefore, the calcination temperatures of 450^{0}C, 550^{0}C, 650^{0}C, and 750^{0}C were selected.

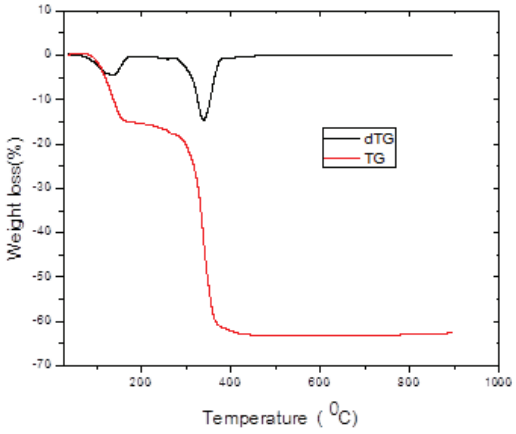

Figure 1. TG-DTG curve of thermal decomposition of zinc acetate dihydrate at heating rate of 10^{0}C in air

The formation of nanosized ZnO can be explained by the following reactions [5] :

$Zn(CH_3COO)_2 + 2H_2O \rightarrow Zn(CH_3COO)_2 + 2H_2O \uparrow$

$4Zn(CH_3COO)_2 + 2H_2O \rightarrow Zn_4O(CH_3COO)_6 + 2CH_3COOH \uparrow$

$Zn_4O(CH_3COO)_6 + 3H_2O \rightarrow 4ZnO + 6CH_3COOH \uparrow$

$Zn_4O(CH_3COO)_6 \rightarrow 4ZnO + 3CH_3COCH_3 \uparrow + 3CO_2 \uparrow$

The XRD patterns of the prepared products were shown in Figure 2. The XRD peaks located at angles (2θ) of 31.8°, 34.4°, 36.2°, 47.5°, 56.6°, 62.8°, 66.3°, 68.1°, and 69.3° corresponding to the (100), (002), (101), (102), (110), (103), (200), (112), and (201) planes of ZnO nanoparticles, respectively. The standard diffraction peaks showed the hexagonal wurtzite structure of ZnO nanoparticles with P63mc space group. The presence of (100), (002), and (101) planes in XRD patterns indicated the formation of highly pure ZnO nanoparticles. Further more, none of the peaks for impurities was observed. Strong intensity and narrow width of ZnO diffraction peaks suggested that the products were well crystalline. The X'Pert High Score was used to further interpret the XRD patterns. Results shown in Table 1 revealed that the characteristic peaks of the synthesized nanoparticles were completely identical to those from the JCPDS data (Card No. 36-1451) [9]. The crystallite size of the nanoparticles was calculated from the peak broadening of diffraction peaks using Debye–Scherer formula $D = \frac{k\lambda}{\beta cos\theta}$, where D is crystallite size, k is constant (0.89), λ= 0.154 nm represents the

wavelength of X-ray radiation, β is the full width at half maximum of diffraction peaks (FWHM) in radian, and θ is the Bragg's angle [6]. The size of the crystallites of ZnO nanoparticles was evaluated by measuring the FWHM of the most intense peak (101) because it had a relatively strong intensity and did not overlap with the other diffraction peaks. Approximately, the average crystallite size of ZnO-450 was of 33nm while those of ZnO-550, ZnO-650 and ZnO-750 were of 36, 38 and 42 nm, respectively. The elevated surface energies at higher calcination temperatures may be responsible for the increasing of the crystallite size. Similar phenomenon was also reported in former studies [1], [4].

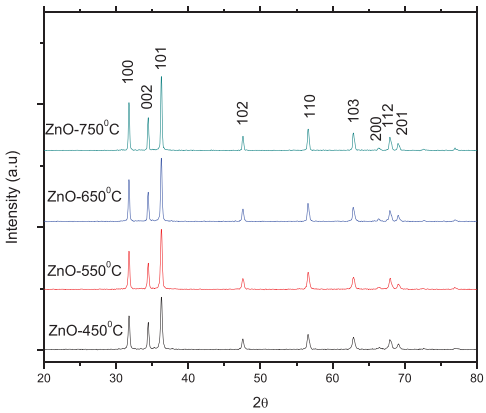

Figure 2. XRD patterns of the nanocrystalline ZnO samples thermally decomposed at 450, 550, 650 and 750^{0}C for 4h

The lattice cell parameters (α and c) of hexagonal wurtzite structure were calculated as the followings [8]:

$$c = \frac{\lambda}{sin\theta_{(002)}} \quad (1)$$

$$a = \frac{\lambda}{\sqrt{3}\, sin\theta_{(100)}} \quad (2)$$

$$\frac{1}{d_{hkl}^2} = \frac{4}{3}\left[\frac{h^2+hk+k^2}{a^2}\right] + \frac{l^2}{c^2} \quad (3)$$

Where d is the interplanar distance; h, k, l are Miller indices of the plane; λ = 1.54 Å is the wave length of the used X-rays; and, θ_{100}, and θ_{002} are angles of the diffraction in degree corresponding to the plane of 100 and 002. The volume (V) of the unit cells of hexagonal wurtzite structure was calculated in the equation:

$$V = 0.866 \times a^2 \times c \quad (4)$$

Results were listed in Table 2 in comparisons with the standard JCPDS data. It was evident that the lattice parameter values of as-synthesized ZnO nanoparticles were similar to the standard values of ZnO. Hence, it could be concluded that the ZnO nanopartilces were well crystalline.

Table 1. Comparison between XRD results of ZnO nanoparticles and standard pattern for ZnO powder

JCPDS (36-1451)			ZnO-450^{0}C			ZnO-550^{0}C			ZnO-650^{0}C			ZnO-750^{0}C		
hkl	2Θ	%I	2Θ	%I	FWHM	2Θ	%I	FWHM	2Θ	%I	FWHM	2Θ	%I	FWHM
100	31,76	57	31,79	64	0.236	31,79	63	0.236	31,79	66	0.207	31,79	64	0.207
002	34,42	44	34,46	51	0.207	34,47	43	0.207	34,43	46	0.236	34,43	44	0.207
101	**36,25**	**100**	**36,28**	**100**	**0.266**	**36,27**	**100**	**0.246**	**36,26**	**100**	**0.230**	**36,26**	**100**	**0.207**
102	47,53	23	47,56	20	0.266	47,54	17	0.325	47,59	20	0.236	47,59	19	0.236
110	56,60	32	56,58	28	0.236	56,62	28	0.325	56,55	27	0.207	56,55	27	0.295
103	62,86	29	62,87	22	0.354	62,78	16	0.236	62,83	21	0.266	62,83	20	0.207
112	67,96	22	67,94	17	0.413	67,99	18	0.207	67,93	17	0.413	67,91	17	0.354
201	69,09	16	69,14	10	0.360	69,10	9	0.413	69,08	9	0.236	69,05	9	0.207

Table 2. Estimated structure parameters and average crystallite size of ZnO nanoparticles from the XRD data

Samples	a (Å)	c (Å)	c/a	Volume of unit cell ($Å^3$)	Size of the crystallites (nm)
JCPDS 36-1451	3.249	5,205	1.602	47,58	x
ZnO-450^{0}C	3,246	5,199	1,602	47,44	33
ZnO-550^{0}C	3,246	5,198	1,601	47,43	36
ZnO-650^{0}C	3,246	5,203	1,603	47,48	38
ZnO-750^{0}C	3,246	5,203	1,603	47,48	42

The surface morphology and size of ZnO nanoparticles were imaged using FESEM analysis (Figure 3). Both spherical like (diameters of 40-100nm) and rod-like (diameters of 50-200nm and lengths of 200-500nm) ZnO nanoparticles were produced. Calcination temperatures were found to dramatically affect the morphology of the nanoparticles formed. At the temperature of 450°C, the rod-like particles were predominant. Nevertheless, more spherical like particles were formed as the temperatures raised. This was clearly confirmed by transmission electron microscopic (TEM) analysis (Figure 4).

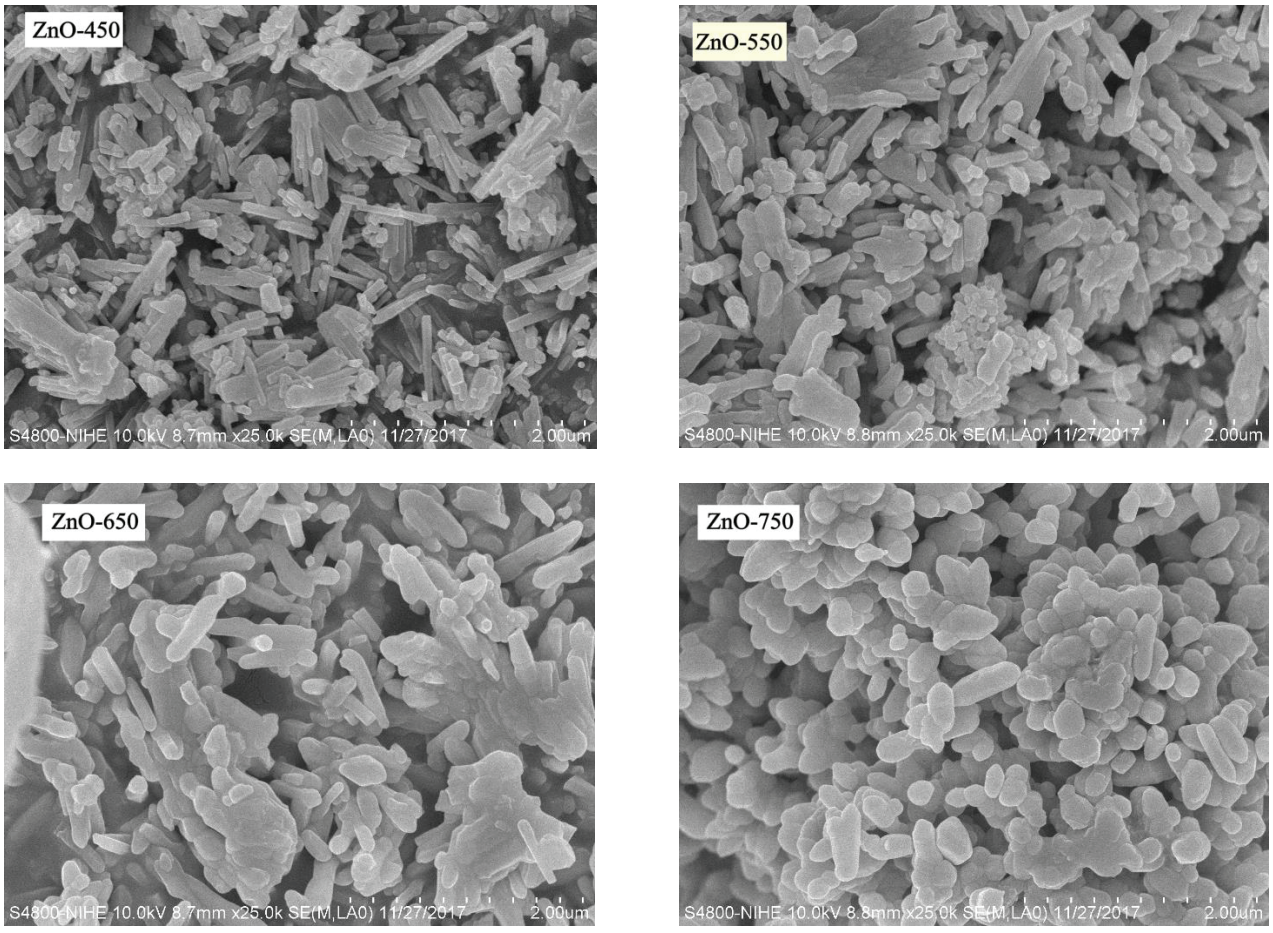

Figure 3. FESEM images of the ZnO nanoparticles thermally decomposed at 450, 550, 650 and 750^{0}C

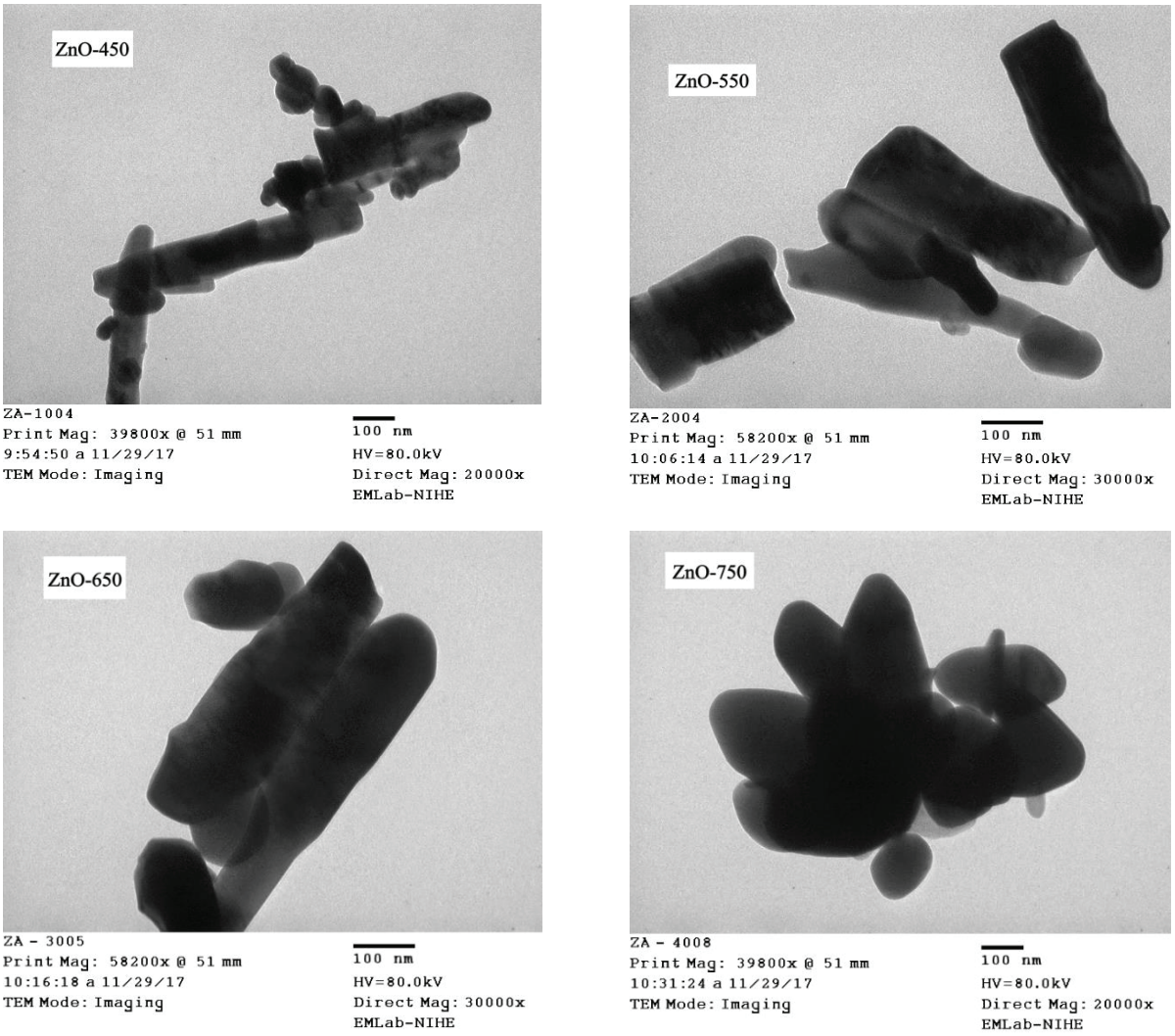

Figure 4. TEM images of the ZnO nanoparticles thermally decomposed at 450, 550, 650 and 750^{0}C

Conclusion

The nano-sized ZnO particles were successfully generated by a direct simple, fast and eco-friendly thermal decomposition route of zinc acetate without additional chemical reagents. The XRD results revealed that ZnO nanoparticles had wurtzite structure. The FESEM, TEM analysis showed both rod-like and spherical like morphology of the nanoparticles. The morphology and size of the nanoparticles were strongly affected by calcination temperature.

Acknowledgments

The authors would like to thank the Ministry of Science and Technology in South Korea through the International Environmental Research Institute (IERI), Gwangju Institute of Science and Technology (GIST) for providing financial assistance for this research project.

References

1. Agnieszka Kołodziejczak Radzimska.; Teofil Jesionowski, Zinc Oxide—From Synthesis to Application: A Review, Materials (2014), 7, 2833.
2. Udayabhanu, G. Nagaraju, H. Nagabhushana, R. B. Basavaraj, G. K. Raghu, D. Suresh, H. Rajanaika, and S. C. Sharma, , Green, Nonchemical Route for the Synthesis of ZnO Superstructures, Evaluation of Its Applications toward Photocatalysis, Photoluminescence, and Biosensing, Crystal Growth & Design, (2016), 16 (12), pp 6828–6840

3. Kezhen Qi, Bei Cheng, Jiaguo Yu, Wingkei Ho, Review on the improvement of the photocatalytic and antibacterial activities of ZnO, Journal of Alloys and Compounds 727 (2017) 792-820.
4. Sotirios Baskoutasa, Panayotis Giabouranis, Spyros N.Yannopoulos, Vassilios Dracopoulos, LajosToth, Athanassios Chrissanthopoulos, Nikolaos Bouropoulos (2007), Preparation of ZnO nanoparticles by thermal decomposition of zinc alginate, Thin Solid Films Volume 515, Issue 24, Pages 8461-8464
5. Chih-Cheng Lin, Yuan-Yao Li (2009), Synthesis of ZnO nanowires by thermal decomposition of zinc acetate dihydrate, Materials Chemistry and Physics 113 , 334–337
6. Ravi Shankar, Rajneesh K. Srivastava, and S. G. Prakash (2013), ZnO NPs synthesized by thermal decomposition of zinc oxalate at 300°C and its photo response under UV-illumination, AIP Conference Proceedings 1536, 239
7. Mutasim I.Khalil, Maha M.Al-Qunaibit, Aisha M.Al-zahem, Joselito P.Labis (2014), Synthesis and characterization of ZnO nanoparticles by thermal decomposition of a curcumin zinc complex, Arabian Journal of Chemistry Volume 7, Issue 6, Pages 1178-1184
8. M.Kahouli, A.Barhoumi, Anis Bouzida, A.Al-Hajry, S.Guermazi, -Structural and optical properties of ZnO nanoparticles prepared by direct precipitation method, -Superlattices and Microstructures 85 (2015) 7-23.
9. Joint Committee for Powder Diffraction Society (JCPDS), Powder Diffraction Database, Pattern: 36-1451.
10. J.N.Hasnidawani, H.N.Azlina, H.Norita, N.N.Bonnia, S.Ratim, E.S.Ali, Synthesis of ZnO Nanostructures Using Sol-Gel Method, Procedia Chemistry 19 (2016) 211-216.
11. T.P. Rao, M.C. Santhosh kumar, A. Safarulla, V. Ganesan, S.R. Barman, C. Sanjeeviraja, -Physical properties of ZnO thin films deposited at various substrate temperature using spray pyrolysis, Physica B: Condensed Matter 405 (9) (2010) 2226-2231.
12. K. PradeevRaj, K.Sadayandi, (2016) -Effect of temperature on structural, optical and photoluminescence studies on ZnO nanoparticles synthesized by the standard co-precipitation method, Physica B: Condensed Matter, 487 1-7.